PHYTOREMEDIATION OF SEWAGE WATER USING AG/FE ALLOYS SYNTHESIZED BY USING GREWIA OPTIVA LEAF EXTRACT

SEHRISH ASAD¹, WAHEED MURAD¹*, NATASHA ANWAR ², MOHIB SHAH¹, MUHAMMAD HAMAYUN¹, ABDULWAHED FAHAD ALREFAEI³, EMAN ALSHEHRI³, AND SAJID ALI⁵*

¹Department of Botany, Abdul Wali Khan University Mardan, Mardan, KP, 23200, Pakistan
²Department of Chemistry, Abdul Wali Khan University Mardan, Mardan, KP, 23200, Pakistan
³Department of Zoology, College of Science, King Saud University, Riyadh 11451, Saudi Arabia
⁴Central Research Laboratory, King Saud University, Riyadh, Saudi Arabia
⁵Department of Horticulture and Life Science, Yeungnam University, Gyeongsan 38541, Republic of Korea
*Corresponding author email: sajidbioali@gmail.com; waheedmurad@awkum.edu.pk

Abstract

Plants and nanoparticles are essential for efficiently eliminating heavy metals from contaminated soil and water. Current study is designed to biosynthesize silver iron nanoparticles and their alloys using *Grewia optiva* leaf extract. The fabricated alloys were optimized using various parameters i.e. temperature, pH, salt concentration, time optimization and nanoparticles concentrations. The bimetallic nanoparticles were subjected for different analysis and alloys were further characterized for phytoremediation. The effects of Ag/Fe alloys on photosynthetic pigments, phytochemicals, lead (Pb) accumulation and plant development were examined in the hydroponic study conducted on *Brassica campestris*. Seedlings were grown in a combination of Pb-polluted media and wastewater, with an addition of 50mgL⁻¹ of Ag/Fe alloys. Plant tissues were tested for Pb levels using atomic absorption spectrophotometry. Wastewater and Pb had a detrimental effect on the growth of seedlings, but the addition of bimetallic nanoparticles, or alloys, reduced stress and increased plant growth as well as levels of carotenoid and chlorophyll. Plant growth was decreased by Pb at a concentration of 50mgL⁻¹, as well as phytohormones and secondary metabolites. On the other hand, oxidative stress was decreased by treatment with biofabricated bimetallic particles, which enhanced the synthesis of primary and secondary metabolites. Treatment of *B. campestris* roots and shoots with alloys decreased Pb concentrations, whereas wastewater raised Pb levels. These results underlined the promise of nanophytoremediation, reflecting that plants can efficiently remove heavy metals from contaminated water when exposed to suitable concentrations of Ag and Fe nanoparticles and their composites (alloys).

Key words: Bimetallic nanoparticle; Phytoremediation; Spectrophotometry; Heavy metals; Brassica campestris.

Introduction

Nanotechnology has a huge potential to improve water and wastewater treatment because it offers potential benefits like low cost, reuse and high efficiency in removing and recovering the contaminants. Different approaches in the field of nanotechnology are now increasingly used in the treatment of water and wastewater. Nanoparticles are the materials that have at least one dimension smaller than 100 nm. In addition to their bulk characteristics, materials acquire additional size-dependent features at the nanoscale, such as a high surface-to-volume ratio, reactivity, rapid dissolution, and adsorption. These characteristics are applied to the surroundings, proper hygiene, and efficient water treatment (Cruz et al., 2020). By combining nano-remediation and phytoremediation, a process known as nano-phytoremediation, the toxicity of dangerous metals and metalloids in the environment is successfully decreased. Utilizing nano-sized particles (NPs) such as silver and iron improves remediation through surface area enhancement, chemical process promotion and chemical detection of hazardous materials (Azmat et al., 2023). Because of their large surface areas and adsorption abilities, nanomaterials become a practical choice for cleaning up soil. Bimetallic nanoparticles (NPs) synergistically enhance the physical and chemical properties of both constituent metals by combining their respective qualities. Hetero structures, alloyed or intermetallic structures and core-shell structures are the three groups into which they are divided. Although they

were discovered later, bimetallic nanoparticles are presently a fascinating area of research because they allow for the flexible modification of particle properties through the combination of two metals, thereby increasing their applications in imaging, biology and catalysis including electrocatalysis (Loza *et al.*, 2020).

Ecosystems are under serious threat from contamination by heavy metals which could come from various sources like inappropriate agricultural practices and uncontrolled industrial /urban waste dumping sites. Heavy metal pollution is not just detrimental to soil but also extremely harmful for water resources especially around agricultural fields where toxic metals tend to accumulate thus pose health risks through the food chain. However, current heavy metal clean-up methods have both pros and cons so, new ideas are required if progress is to be made. Other alternatives include phytoremediation using plants or bioremediation through biological agents that break down wastes. This novel approach of using hyper-accumulating plants in particular has been found to be cost effective, environmentally friendly, long-term and advanced method of cleaning up metal contaminated areas by phytoremediation. Currently used in a wide range of industries, including paints, textiles, pharmaceuticals, and cosmetics, nanomaterials are also essential environmental remediation because they pollutants from the air, water, and soil (Sharma et al., 2022). The intake of pollutants in soil and mineral water is posing a intense danger to public health and is considered as one of the biggest issues worldwide.

The current study has been focused on the phytoremediation process utilizing the greenly synthesized nanoparticles and their alloys. The research work will be helpful to understand the overall functions of metal nanoparticles and their alloys remediating contaminated soils. The use of plants as a reducing agent is providing ecofriendly and a very easy route to synthesize metal nanoparticles, as the reduction process initiates within a short time in comparing physico-chemical synthesis. No literature has been found on the Grewia optiva plant regarding the synthesis of nanoparticles and their composites. This research study will provide a baseline way to utilize the Grewia optiva as a reducing agent and it will pave a way for a new research approach to produce an ecofriendly absorbent. The research study may be helpful to focus on a well efficient system for eliminating pollutants and documentation in the relevant field for future research.

Material and Method

Collection and cleanliness of the fresh leaves: Fresh leaves were collected from *Grewia optiva* plant, washed with clean tap water, shade dried, powdered and used for the research work (Arshad *et al.*, 2022). The plant specimen of the collected leaves was identified with help of available literature (Asad *et al.*, 2022). The Plant specimen has been assigned a voucher specimen no. Awkum.Bot.75.2.1 and deposited in the herbarium, AWKUM.

Extraction of plant aqueous extract: 25gm powder of leaves was mixed with 100mL distilled water. The mixture was placed in a jeldal apparatus at a temperature of 60°C to boil for 20 minutes. Then, the samples were filtered using Whatman paper. The filtrate was subsequently placed in a refrigerator for future use (Asad *et al.*, 2022).

Biosynthesis of Ag/Fe alloys: A mixture of 1mM solution of each AgNO₃ and FeCl₃ with *Grewia optiva* leaf extract was placed on magnetic stirrer for 24 hrs. UV-Spectrometry was used for all samples upon complete reduction (Xu *et al.*, 2022).

Optimizations

Synthesized alloys of Ag/Fe were optimized by time duration (synthesis time). For this purpose, samples were optimized for 30 min, 60min, 90 min and 24 hrs. After completion of time duration all samples were assessed respectively for absorbance using UV- spectroscopy. For optimizing temperature effects on synthesized Ag and Fe Alloys, a range of different temperature ranges (From room temp to 95°C) was used correspondingly for ten minutes to measure the absorbance by using UV-spectrometery (Asad et al., 2022). Optimization of salt concentration effect was carried out on synthesized alloys. 1mM solution of NaCl was prepared and added to each alloys solution absorbance using UVrespectively to check the spectrometry (Anwar et al., 2022). 0.1N solution of NaOH and HCl were prepared to optimize pH effect on silver iron alloys. pH of the solution was adjusted as pH1-2, pH 2-3, pH 3-4, pH 4-5, pH 7- 8, pH 8-9, 10 and pH 11-12 corrispondingly. UV- spectroscopy technique was used to measure absorbance of all samples (Anwar et al., 2022).

Characterization

UV-vis Spectroscopy: The absorbance of biofabricated silver, iron nanoparticles and their alloys of *G. optiva* plant were analyzed using UV-Spectroscopy. Distilled water has been used as a control to evaluate the absorbance of mono and bimetallic nanoparticles. The formation of individual nanoparticles and their alloys were examined using a UV-1602 double beam UV-vis spectrometry with a resolution of 1 nm. A leaf extract and salt were utilized to measure the spectrum absorbance for nanoparticles fabricated by reaction mixtures. Solutions of silver nitrate and iron (III) chloride hexahydrate were used in ratio of 1:1 to 1:6 with a ranging of 300-800 nm wavelength (Acay *et al.*, 2021).

FT-IR Spectroscopy: The alloys were dried at a temperature of 37°C using a vacuum dryer, the nanoparticles were mixed with KBr and compressed (hydraulic pellet press). FT-IR SPECTRUM ONE was used for all the samples FT-IR spectroscopy, having a resolution of 4 cm⁻¹ with a range of 4000cm⁻¹ followed by the *G. optiva* leaf extract for analysis of nanoparticles by using the same method and same technique (Acay *et al.*, 2021).

X-Ray Diffraction (XRD) Analysis: The X-ray diffraction pattern of silver iron alloys of *G. optiva* leaf extract was examined using JEOL JDX 3532 X-ray diffract meters. The nickel monochromator filtering the wave at a tube voltage of 40KV and a tube current of 30mA with Cu-K radiation was used to note the diffraction patterns of biofabricated nanoparticles (Acay *et al.*, 2021).

Scanning electron microscopy: The vacuum-dried silver iron alloys were put onto a carbon-coated SEM grid, dried and then metalized with a Spi-module sputter coater to provide metal coating on them. The morphological features of the metal coating were also investigated by FE-SEM (JSM-5910-JEOL) and scanning electron microscopy (Mofolo *et al.*, 2020).

Transmission electron microscopy (TEM): The alloys (nanocomposites) were mixed with KBr and pressed into sample pellets using a water pellet press and then the size of the biofabricated alloys was determined by transmission electronically transmission microscopy (TEM).

Environmental management

Wastewater collection: Wastewater was collected from the community sewage system in Mardan located in the vicinity of Abdul Wali Khan University, Mardan (AWKUM) and stored in plant biology laboratory of Department of Botany, AWKUM.

Physicochemical characterization of waste water: Using a standard protocol, measurements of a variety of parameters of physic-chemical properties of waste water were made, these are including pH, turbidity, temperature, biological oxygen demand (BOD5), ions, dissolved oxygen (DO), iodine, aluminum, silica, ammonia, zinc, etc. A multi-parameter photometer and COD were used to conduct different metal tests such as Free Chlorine,

Aluminum, Ammonia, Bromine, Copper, Cyanide, Nickel, Chromium, Iron, Magnesium, Nitrate, Zinc, Alkalinity and water colour. (Nizam *et al.*, 2022).

Seeds collection and transplantation: Seeds of Hasnain 2013 variety of *Brassica Campestris* L. were soaked in water for about 30 minutes. These seeds were sterilized in ethanol (70%) and washed with water before use. Experiment was conducted to use five replicates in each sample with a total number of 15 seeds to each plate. Fifteen healthy seeds were transferred in each petri dish with five replicates of each concentration. A total of nine concentrations for alloys particles were used and whole experiments were repeated five times.

Nanoparticles and wastewater treatment: The treatments were applied by using hydroponic experiments. Plates were labeled as: Lead (Pb), Wastewater (WW), Tap water (TP), Nanoparticles (NP), Nanoparticles + Wastewater (NW), Tape water and lead (TPPb), Wastewater and Lead (WWPb) Nanoparticles, Wastewater and Lead (NWPb) Nanoparticles and Lead (NPPb).

Application of alloys nanoparticles: Alloys of various concentrations of silver iron nanoparticles were subjected to the seedlings. Growth media was sonicated for 30 min to obtain aqueous suspensions of nanoparticles (Hussain *et al.*, 2021).

Growth media and addition of lead: Hoagland's solutions as growth media was used for all the hydroponic culture's growing media and lead was added to the media prepared by following the standard procedure in the form of concentration of 50mgL-1 and were mixed (Hoagland, 1950).

Plant harvesting and data collection: After 30 days of treatment, plants were properly harvested and cleaned with 5Mm EDTA solution to remove surface bounded impurities. Root shoot length and fresh/Dry weight were measured using standard protocol of Hussain *et al.*, 2012.

Phytochemical screening of plant metabolites: Quantitative estimation of various plant metabolites i.e., phenols, total chlorophyll, phytohormones (IAA, ABA, GA₃) H₂O₂, Lipids, peroxidase, catalase were evaluated using standard protocols.

Extraction and estimation of total chlorophyll: Estimation of total chlorophyll in *B. campestris* were carried out using protocol Maclachlan *et al.*, 1963. Leaves of *B. campestris* were collected and crushed in 3cc of 80% acetone. The solutions were centrifuged and supernatant were added with 7mL of 80% acetone. Optical densities for chlorophyll a at 663nm, for chlorophyll b 645nm, for carotenoids and xanthophyll at 480nm and 510nm respectively were calculated using V-1100 Spectrophotometer.

Estimation of protein: Protocol was followed to estimate the level of protein in *B. campestris* leaves (Lowry *et al.*, 1951). Four different reagents (A, B, C, D) were prepared for the protein test following the protocol.

Reagent A: 100mL of DW were mixed with KNaC₄H₄O₆-H₂O (1gm) and 2 gm of Na₂CO₃(2gm)

Reagent B: 0.5gm CuSO₄.5H₂O was added to 100mL of

distilled water.

Reagent C: Reagent A (50 mL) and reagent B (1 mL)

were mixed.

Reagent D: Reagent D was formed by Combination of

DW and Folin reagent in 1:1.

Procedure: 0.1g of *Brassica* leaves were homogenized with 1 mL of KH_2PO_4 & K_2HPO_4 buffer (0.1 M, pH=7) in ice-chilled mortar. Samples were refrigerated and then centrifuged for 10 minutes at 4000 rpm. After centrifugation 0.1mL of supernatant was mixed to Distilled water to raise the volume upto 1mL for each sample. After mixing with DW Reagent C was combined to the sample and kept for ten minutes and then Reagent D was mixed with the sample and incubated for thirty minutes. The samples were then subjected for calculation of optical density at 650nm using V1100 Spectrophotometer.

Estimation of sugar: Fresh leaves (0.5g) were homogenized with distilled water and the samples were centrifuged. The supernatant was mixed with sulfuric acid (98%) and phenol (5%). All samples were incubated for 60 Minutes. After incubation the absorbance of the reaction mixture was determined at 480 nm using V-1100 spectrophotometer. The Benedict solution was used to quantify the sum total of sugar present in *B. campestris* as a blank(Heidari *et al.*, 1951).

Estimation of phytohormones

Estimation of indole acetic acid (IAA): Salkawaski reagent was prepared by mixing 8mL of 0.5M FeCl₃+49mL of 70% HCLO4 + 49mL DW. Leaves aqueous extract were prepared and centrifuged at 10,000 rpm. 1mL of supernatant were combined with 2mL of Salkawaski reagent and incubated for 30 minutes at room temperature in the dark. Absorbance of all samples was measured at 540nm using UV-spectrophotometer. Salkawaski reagent was used as a blank in the reaction.

Estimation of ABA and GA3: For determination of ABA and GA3 in leaves, Combine solution were prepared by adding **Methanol** (12mL): Chloroform (5mL): 2Nammoniumhydroxide (3mL). Combine solution was stored at -20°C.

Procedure: 1g of fresh leaves were combined in 5mL of combine solution. Combine extract were mixed with 25mL distilled water due to chloroform phase appeared. Chloroform phase was discarded. After chloroform phase removal, methanol and water phase were evaporated. Then 1.5mL of ethyl acetate was added to the reaction mixture and samples were incubated for 1hr at 70°C. After incubation ethyl acetate were evaporated at 45°C on rotary-evaporator. After completion of procedure samples were subjected to measure absorbance for GA₃ at 254nm and for ABA 263nm. Combine solution was used as a blank in the test (Ismail *et al.*, 2020).

Estimation of lipids: For estimation of total lipids in *B. campestris* leaves Reagent Vanillin- phosphoric acid was used. Vanillin (600mg) were dissolved in hot water (100mL). 400mL of 85% of phosphoric acid were added to the mixture and stored in the dark.

Procedure: Plant extract were transferred to beaker and allowed to evaporate at 50-60°C. And then concentrated sulfuric acid(5mL) was mixed with the samples and kept for 10 minutes to boil, and then cooled the sample at room temperature. From the reaction mixture 0.2mL was transferred to the test tube and phosphor-vanillin (2.4mL) were combined to the test tube containing sample. Test tube were shaked well and subjected for incubation for an hour. Chloroform (0.2mL) and phosphor- vanillin (5 mL) reagent were combined and used as a blank. Optical density of all samples was measured at 490nm using V1100-Spectrophotometry (Handel *et al.*, 1985).

Estimation of electrolytic leakage: Electrical conductivity of plant samples was evaluated using EC meter. In the first step electrical conductivity value of all samples were measured and then samples were given temperature of 100°C for five minutes. After temperature treatment EC value were again recorded. Electrical conductivity of all samples was recorded using following formula:

EL= EC1/EC2 *100

Determination of catalase: Reaction mixture for required enzymatic test were prepared by combining 0.2mL of enzyme extract, 2mL of phosphate buffer having pH-7.0 and 3% of H₂O₂. Samples were further used to determine the OD at 240nm using Spectrophotometry. Phosphate buffer was used as blank in the reaction (Mavelli *et al.*, 1982).

Determination of peroxidase: 0.3g of fresh leaves was homogenized in phosphate buffer having 6.8 pH. After complete homogenization samples were centrifuged at 13500 rpm for 13 minutes and supernatant was separated from the pellet. Supernatant was mixed with 50μ L pyrogallol, and with 50μ L H₂SO₄. Samples were incubated for 5 minutes at 25°C. After incubation 0.5mL of H₂SO₄ were added to the reaction mixture. All samples were further used to determined absorbance at 420nm using V1100-Spectrophotometry(Gorin & Heidema, 1976).

quantification using atomic absorption spectrophotometry: Dry samples of root and shoot (0.5 gm each) were crushed and used for digestion; each plant sample received 6.5 mL of acid solution viz. HNO₃, H₂SO₄, HCLO₄ in a 5:1:0.5 ratio to be digested; samples were soaked for 12 hours; following the soaking period, the samples were heated for approximately 3 hours at 300°C until white vapors formed. The various lead concentrations in the dried and powdered Brassica campestris L. samples were assessed. Before being filtration, the samples were dilute with distilled water. An atomic absorption spectrophotometer (AAS 4000) was utilized to determine the quantity of heavy metals (Khan et al., 2021).

Results

Synthesis of alloys: Silver and iron nanoparticles were prepared using the leaf extract of *G. optiva* and their synthesis was confirmed by appearance of brown coloration with absorbance peak of 413nm and greenish black color having absorbance peak at 270nm respectively. Solutions (AgNPs and FeNPs) were mixed with each other in various ratios. The maximum peak absorbency was calculated in 4:1 (Ag:Fe), having two peaks i.e., 403nm for silver and 269nm for iron. The result demonstrated that 4:1 concentration is favorable for fabrication of alloys using silver iron nanoparticles (Fig. 1).

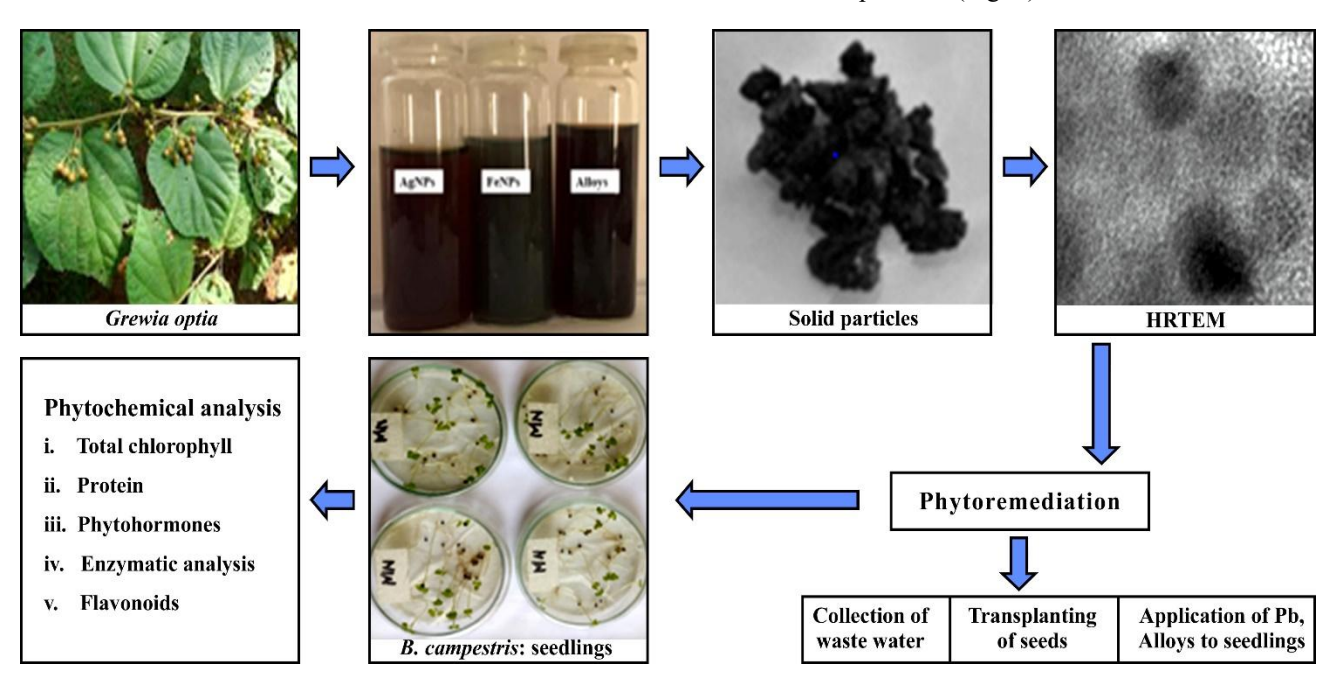


Fig. 1. Overview of research work.

Optimization: pH, temperature, volume, time duration, salt concentration and molar concentration are essential for controlling the size of nanoparticles in their synthesis process. The findings showed that at a 4:1 volume ratio (Ag: Fe), where peaks corresponding to both particles were seen within their respective wavelength ranges, the ideal chemistry for iron and silver in Ag/Fe alloys was reached (Fig. 2). The absorbance peaks decreased in acidic pH and increased in basic pH (Fig. 2C). Result showed that alloys synthesis was enhanced as pH level was increased, i.e maximum peak was observed by basic pH while peak deacresed at acidic pH. Peak absorbency was decreased as salt concentration increased i.e., highest peak was observed at 0.2mL while minimum peak was observed at 1mL of salt concentration showing that high salt concentration despite the decrease in the rate of synthesis (Fig. 2D). For instance, the effects of temperature on synthesis of alloys were also evaluated. Initially as temperature increased, rate of absorbency was also followed by a progressive decrease between 65°C to 80°C as indicated by UV spectra. This temperature range reflects that alloy synthesis had been optimized as depicted by greatest absorption (Fig. 2E).

Time duration optimization was also evaluated for the synthesized composite of Ag/Fe particles. Various time parameters were tested, and UV measurements were taken upon completion of each respective time duration. The alloys exhibited the highest peak at the 3-hour mark, confirming the significant role of time optimization in the controlled synthesis of Ag/Fe alloys (Fig. 2F).

Characterization

Fourier transforms infra-red spectroscopy: Silver, iron nanoparticles and their alloys were analyzed by using FTIR spectroscopy (Fig. 3). Absorbance peaks of the leaf extract has been examined at 3269, 2919, 2843, 1955 and 1630 cm⁻¹ with the high shift at 3269 cm⁻¹ to correspond with the primary amines N-H group, 2919 cm⁻¹ with the C-H bond, 2843 cm⁻¹ with the C-H bond in alkanes, 1955 cm⁻¹ with the C-H bond, and 1630 cm⁻¹ for the C=C bond. Bands of FeNPs are shown at 3278, 2919, 2168, 1638, and 1545 cm⁻¹ corresponding to N-H group, C-H bond, O-H, C=C and alkanes respectively. The alkanes bond with a shift to 1955cm⁻¹ was examined in FTIR peak of AgNPs.

Ag/Fe alloys' FTIR spectroscopy has shown shifts at 3278, 2936 and 1528 cm⁻¹ corresponding to the nitro compounds N-H bond, C-H bond, and N-O respectively. Such shift bands were also seen in the FTIR analysis of the alloys, further confirming the existence of Ag and Fe in the alloys (Fig. 3) (Asad *et al.*, 2022).

X-ray diffraction (XRD): Ag/Fe alloys were analysed by utilising XRD to confirm their crystalline nature. Bragg's representation confirms face centered cubic structure of prepared alloys and diffraction peaks at 38.28°, 46.63°, 64.81° and 72.27° during crystallographic representation. These peaks correspond to the planes; 111, 200, 220 and 311 respectively (Fig. 4).

Scanning electron microscopy: At different magnifications, the size, morphology, and shape of the prepared Ag/Fe alloys were assessed using scanning

electron microscopy (SEM). The SEM micrographs showed that alloys in diverse shapes were present. More specifically, during the analysis, rod-shaped, spherical and irregularly shaped particles or aggregations of alloys were seen (Fig. 5A, 5B).

Transmission electron microscopy: High resolution TEM was used for examination of size shape of alloys, along with a histogram morphology. The alloys displayed spherical shape with hexagonal structure. 14-83nm size of prepared alloys were confirmed by TEM (Fig. 5CD).

Phytoremediation: Current research is designed to mediate waste water and lead through nano-phytoremediation. *Brassica campestris* L. plant specimens were used as test plant because *B. campestris* have high potential of phytoremediation. Greenly synthesized and characterized Ag/Fe alloys were utilized to check their effect on *Brassica campestris* remediation properties.

Physiochemical evaluation of collected sewage water: In order to evaluate various physicochemical parameters, wastewater samples were collected from both the Abdul Wali Khan University Mardan campus and its surrounding areas.

Plantation of *Brassica campestris* **seedlings:** For the experiment, hydroponic conditions were used with uniformly sized petri plates. After harvesting, the lengths of the roots and shoots were measured in centimeters, and each plant was weighed, both dry and fresh. The treated plant groups underwent a variety of physicochemical analyses utilizing standard protocols and UV spectrophotometry to evaluate their quantitative attributes (Fig. 6).

Estimation of root and shoot length: The results demonstrated that seedlings treated with alloys induced growth, with better shoot lengths reaching 10.3 cm, but lead (Pb) and wastewater (WW) treatments caused reduced shoot lengths of 4.03 and 6.1 cm, respectively. Furthermore, tap water along with lead and wastewater combined with Pb (TpPb and WWPb) showed shoot lengths of 6.4 and 5.6 cm, correspondingly, while AlWW (Pb) and Alloys (Pb) treatments demonstrated effective shoot lengths of 8.1 and 4.78 cm, respectively. Seedling treated with alloys exhibited the highest root growth (7.3 cm), followed by AlWW with a root length of 5.7 cm. Root lengths decreased to 3 cm, 4.4 cm, and 4.1 cm, respectively, under stress conditions of Pb, TpPb, and WWPb. Nevertheless, root length promotion was seen after the application of alloys, with PbAl reaching 5.1 cm and PbAlWW reaching 4.7 cm (Fig. 7).

Fresh and dry weight: Alloy-treated seedlings had the greatest fresh weight (0.393 g/mg); tap water, wastewater, and lead treatments had fresh weights of 0.08, 0.075 and 0.056 mg/g, correspondingly. The fresh weights of alloys combined with wastewater (AlWW) were lower than those of alloys alone in non-stress situations, but they were greater than those of tap water and wastewater alone. However, under stress conditions caused by the administration of lead, a reduction in fresh weight was seen. AlWW (Pb) and alloys (Pb) demonstrated greater

results at 0.09 and 0.12 g/mg, respectively, whereas Tp (Pb) and WW(Pb) had fresh weights of 0.063 and 0.025 g/mg (Fig. 8). When dry weight was estimated under nonstress, the weights of the alloy-treated seedlings were 0.196 g/mg, greater than the weights of lead, wastewater, and tap water, which were 0.06, 0.018 and 0.07 g/mg,

accordingly. While Alloys(Pb) and AlWW (Pb) demonstrated effective results at 0.065 and 0.0317 g/mg, respectively, WW(Pb) and Tp(Pb) showed dry weights of 0.037 and 0.055 g/mg under stress.

These findings imply that alloys are useful in reducing lead stress and raising *B. campestris* dry weight.

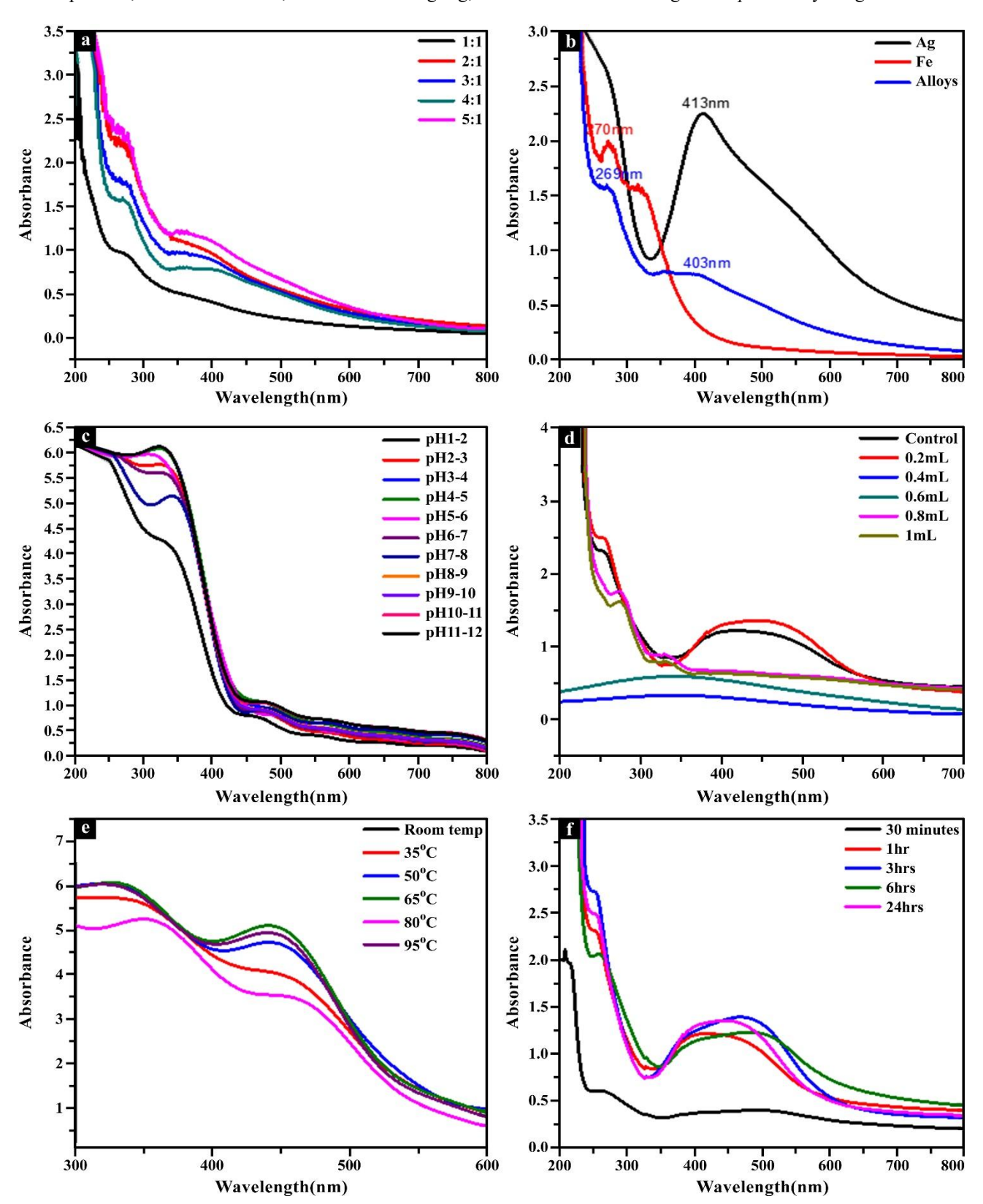


Fig. 2. UV-Spectrophotometry analysis A: Absorbance B: concentration effect(c) pH effect (D) salt effect (E) Time duration effect (F) Temperature effect of Ag/Fe alloys prepared by *G. optiva* leaf extract.

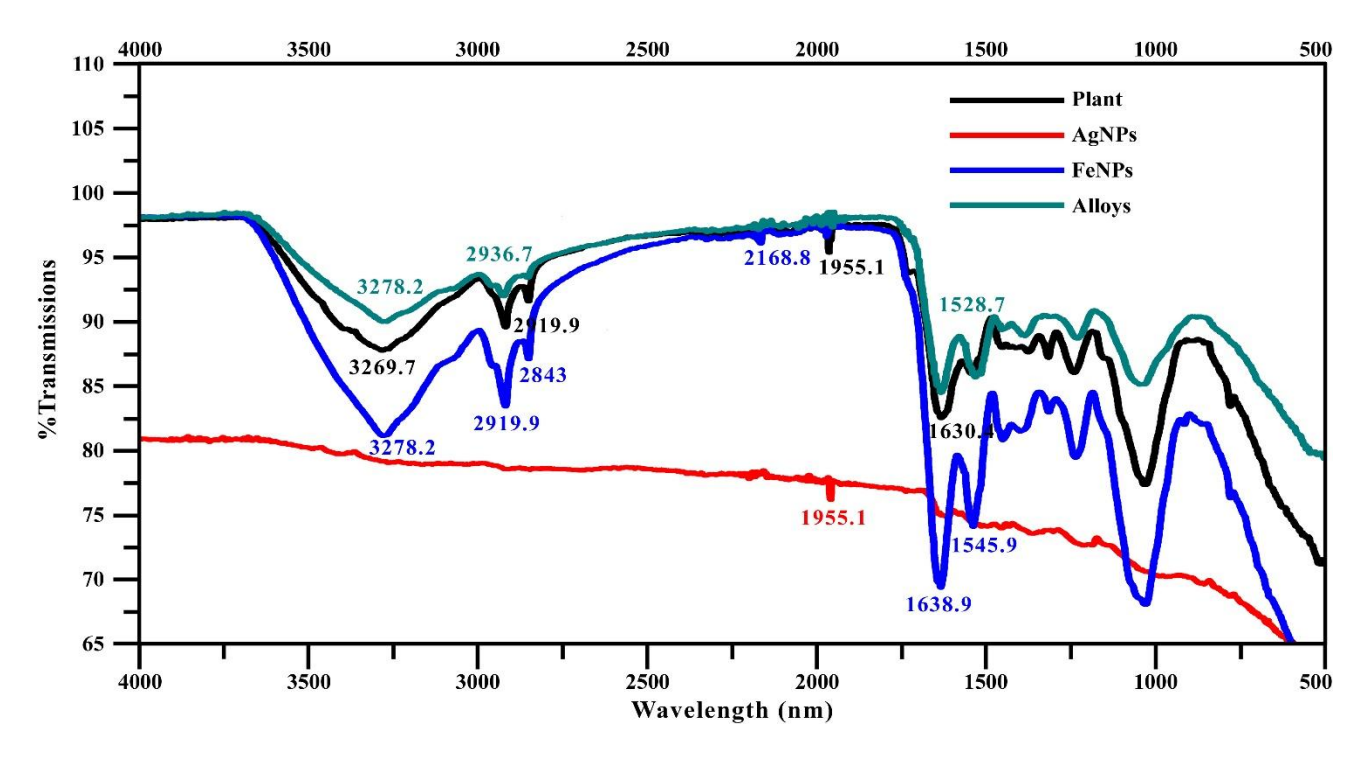


Fig. 3. FT-IR spectroscopy analysis of plant extract, AgNPs, FeNPs and alloys.

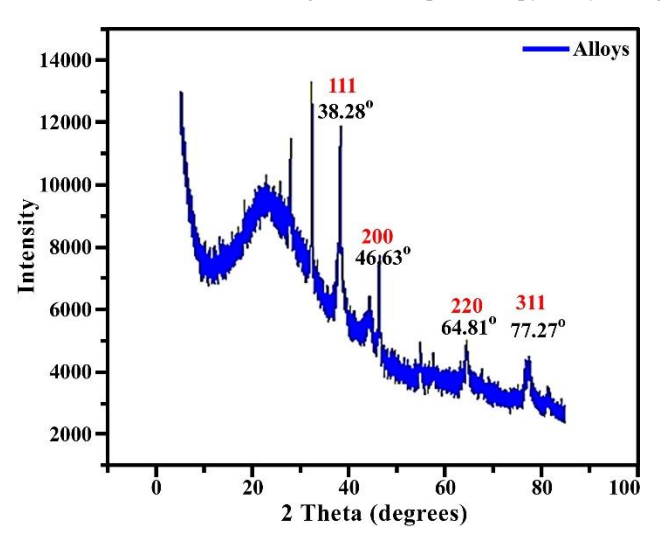


Fig. 4. X-ray diffraction of Ag/Fe alloys.

Quantitative analysis of plant metabolites

Determination of sugar contents: Lead-induced stress conditions led to lower sugar levels; Pb (13 µg/g), WWPb (65 μ g/g), and TpPb (145 μ g/g) of sugar contents were the lowest sugar levels, while the alloys treatment had the highest sugar levels (230 µg/g), followed by WWAI (183 $\mu g/g$) and tap water (179 $\mu g/g$) in the control group. On the other hand, the application of alloys raised the sugar levels in stressful situations. Specifically, the sugar levels for the AlPb and AlWPb treatments were 160 µg/g and 168 µg/g, respectively. Sugar levels decreased under stress conditions caused by lead; Pb had 13 µg/g, WWPb had 65 $\mu g/g$, and TpPb had 145 $\mu g/g$ of sugar content. On the other hand, it has been found that applying alloys led to increase in the sugar levels in stressful situations. In particular, sugar levels were 160 µg/g for AlPb and 168 µg/g for AlWPb treatments, respectively (Fig. 9a).

Determination of protein contents: Alloys were displaying a protein content of 380 μ g/g in the control group whereas 317 μ g/g in tap water. In contrast, waste water had lower (166 μ g/g) protein levels than other treatments. A higher level of protein was recorded in waste water combined with alloys (WWAI). Under stress, Pb (160 μ g/g) and PbWW (126 μ g/g) showed a decrease in protein content. It has been found that tape water + Pb (TpPb) has 280 μ g/g of protein. Furthermore, it was observed that alloys had a larger protein content than any other sample treated under stress. Specifically, alloy+Pb (AlPb) showed a protein content of 320 μ g/g under lead stress (Fig. 9b).

Estimation of Chlorophyll A contents: Compared to all other samples, seedlings treated with alloys showed a higher rate of chlorophyll A content (5.4 mg/g). The seedlings treated with tap water and waste water had chlorophyll a levels of 4.3 mg/g and 3.6 mg/g, respectively. The chlorophyll Under stress conditions caused by lead application, a content level in WW(Pb) and Tp(Pb) decreased to 1.3 mg/g and 3.331 mg/g, respectively, but it increased following alloy treatment. Specifically, it was discovered that the AlPb and AlWWPb treatments had chlorophyll a concentration of 1.6 mg/g and 2.9 mg/g, correspondingly as shown in the (Fig. 10a).

Estimation of Chlorophyll b contents: In particular, alloys with a high concentration of chlorophyll b (17.2 mg/g) were found to have the highest concentration, followed by tap water with 15.1 mg/g. The amount of chlorophyll b in waste water treated with alloys was higher (11.1 mg/g) than in waste water treated without any alloys (5.3 mg/g) in non-stressful conditions; the amount of chlorophyll b in waste water treated with alloys was greater (11.1 mg/g) than in waste water treated without any alloys (5.3 mg/g). Chlorophyll b levels increased to 12.5 mg/g in

alloys+Pb (AlPb) and dropped to 4.8 mg/g in PbWW under lead-induced stress conditions. An average result was observed using TpPb, showing a chlorophyll b level of 7.1 mg/g. Under lead-induced stress conditions, the level of chlorophyll b rose to 12.5 mg/g in alloys+Pb (AlPb) and decreased to 4.8 mg/g in PbWW. With TpPb, an average result was noted, indicating a chlorophyll b content of 7.1 mg/g. Results are presented (Fig. 10b).

Estimation of Carotenoids contents: The findings showed that, of all the samples, the seedlings treated with alloys had the highest carotenoids content (1130 $\mu g/g$). In non-stressful conditions, waste water had a lower carotenoid content (796 $\mu g/g$) than tape water (796 $\mu g/g$). When compared to alloys and tape water, waste water had a lower carotenoid content.

All seedlings' carotenoid content dropped in lead-induced stress conditions. The carotenoid content of waste water plus lead (WWPb) was found to be lower than that of lead alone (193 μ g/g), whereas the highest level of carotenoid content was found in AlPb, which increased carotenoid levels to 360 μ g/g. Under stress, TpPb and AlWWPb displayed carotenoid levels of 630 μ g/g and 400 μ g/g, respectively. (Fig. 10c) provides an illustration of these findings.

Estimation of total Chlorophyll contents: With values of 24.1 mg/g and 18.5 mg/g, respectively, alloys and tape water-treated seedlings showed high levels of total chlorophyll, according to the results. While waste water (WW) treated seedlings displayed a lower level of total chlorophyll (8.5 mg/g) compared to all samples under non-stress conditions, waste water combined with alloys demonstrated a total chlorophyll level of 14.4 mg/g. With values of 8.01 mg/g, 8.56 mg/g, and 10.5 mg/g, respectively, WWPb, Pb, and TpPb were shown to have reduced levels of total chlorophyll under stress. However, under stressful circumstances, total chlorophyll levels increased in response to AlPb (12.8 mg/g) and AlWWPb (9.7 mg/g) treatments as shown in the (Fig. 10d).

Determination of peroxidase in *Brassica campestris*: In particular, peroxidase levels during stress conditions caused by Pb, WWPb, and TpPb treatments were 1.58unit/g, 1.86unit/g, and 1.28 unit/g, respectively. AlPb and AlWPb alloy treatments under stress led to a drastic decrease in their respective values (1.68 and 1.4 units/g) Under non-stress conditions, the alloys' peroxidase content was 0.6 units/g, while that of tap water, AlWW, and WW was 0.8, 0.92, and 0.83 units/g, accordingly. Figure 11a demonstrates the findings.

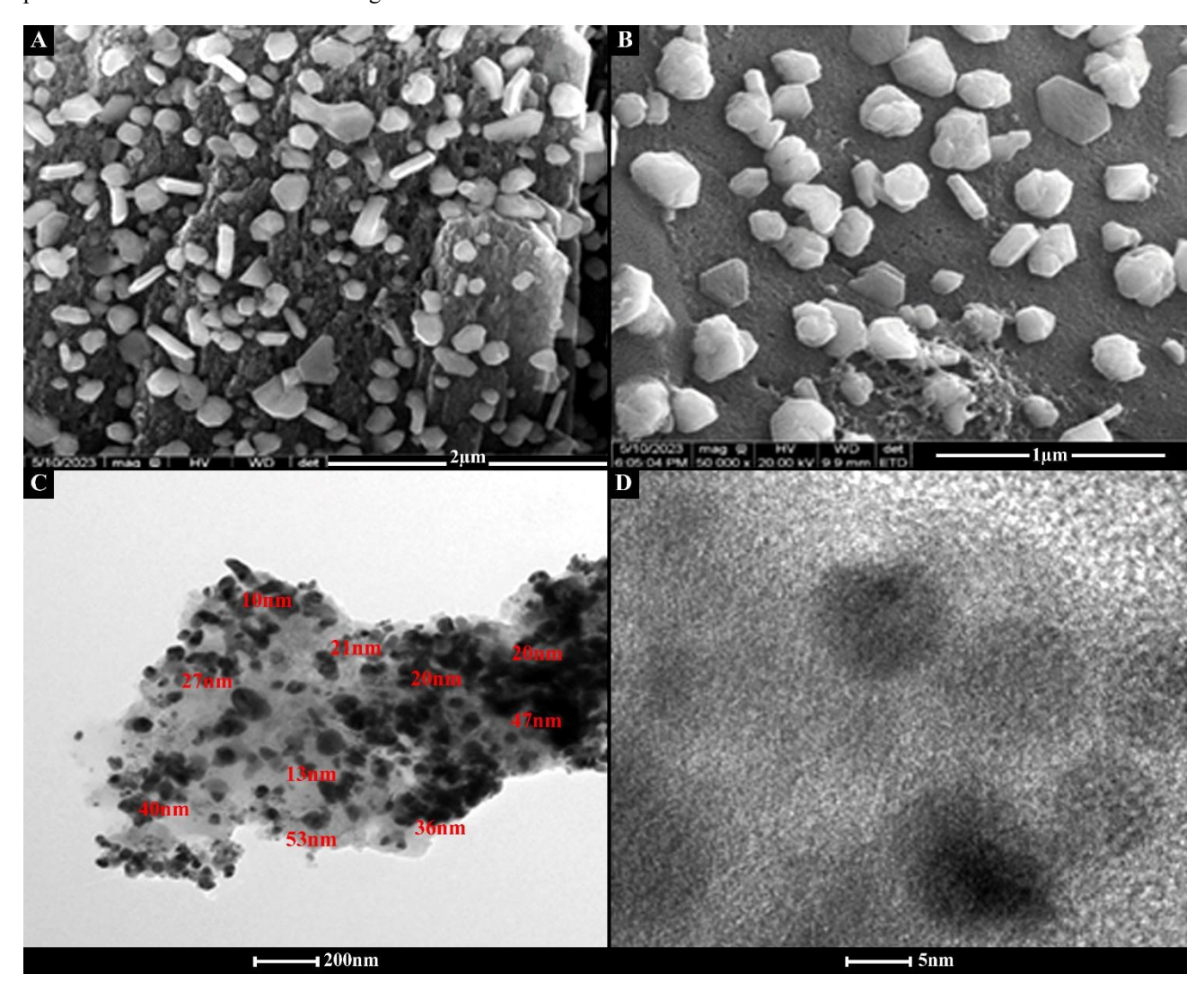


Fig. 5. Micrograph of SEM at (A) magnification of 2μm (B) magnification of 1μm, Micrograph of TEM(C) TEM image at 200nm magnification and histogram (D) HR-TEM of Ag/Fe alloys prepared by *G. optiva* leaf extract.

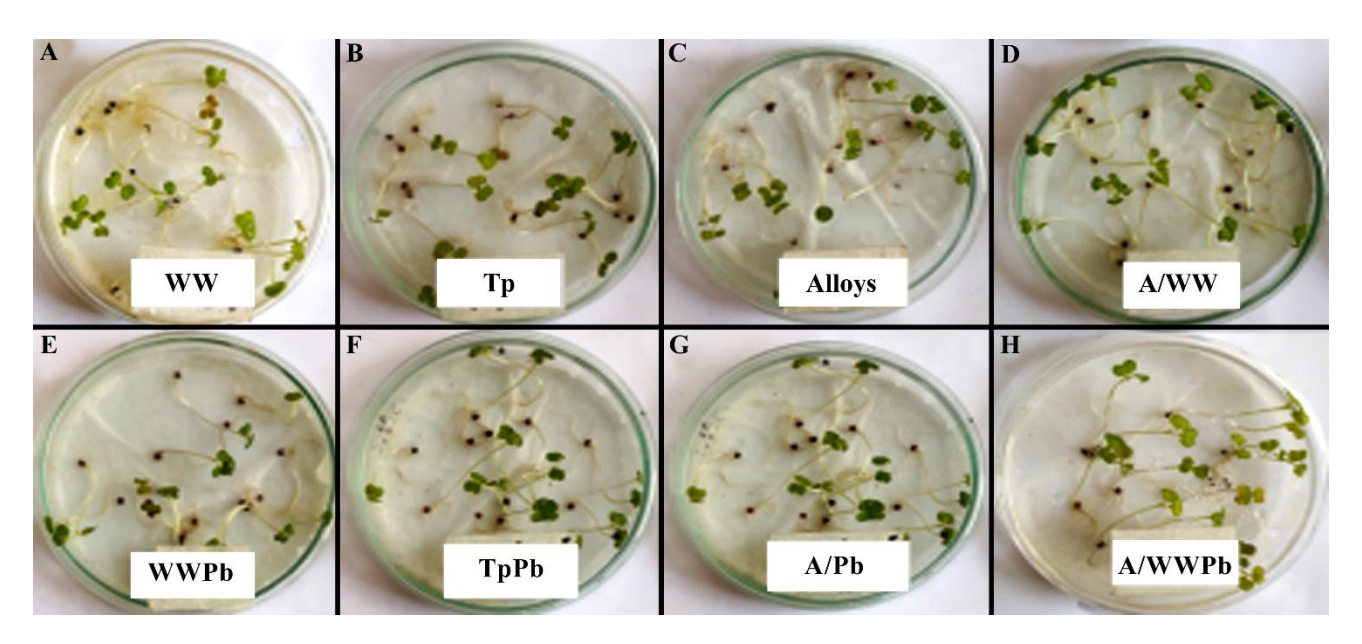


Fig. 6. Hydroponic experiments of *B. campestris* seedlings having treatments of (A) wastewater(B) Tapewater(C). Alloys (D) Alloys + Wastewater (E) Wastewater + Lead (F) Tapewater + Lead (G) Alloys + Lead (I) Alloys + Wastewater + Lead.

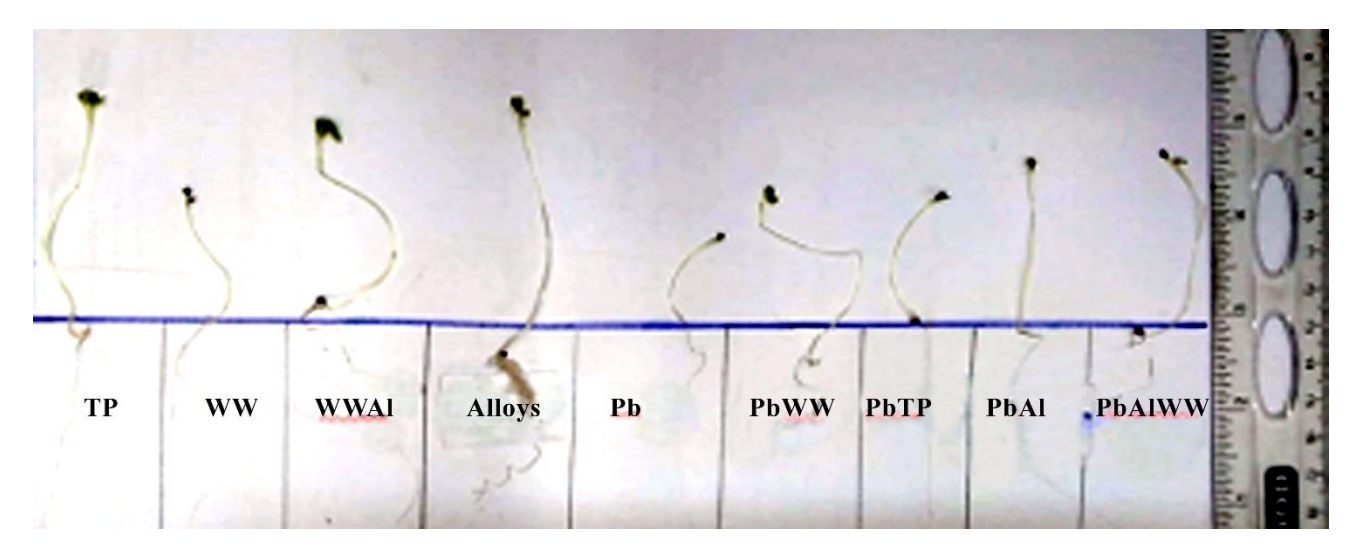


Fig. 7. Growth of Brassica campestris seedlings in control under lead stress.

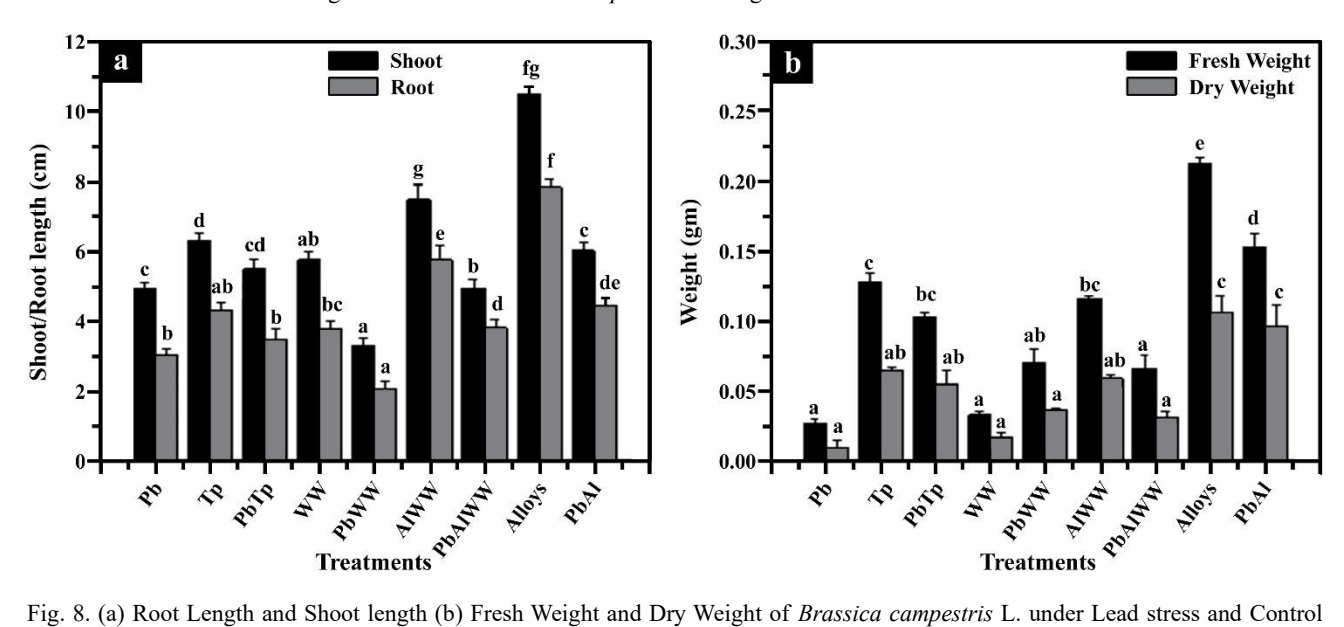


Fig. 8. (a) Root Length and Shoot length (b) Fresh Weight and Dry Weight of *Brassica campestris* L. under Lead stress and Control condition. Each bar represents the tripled data's mean along with its standard error with significant rate of p < 0.05.

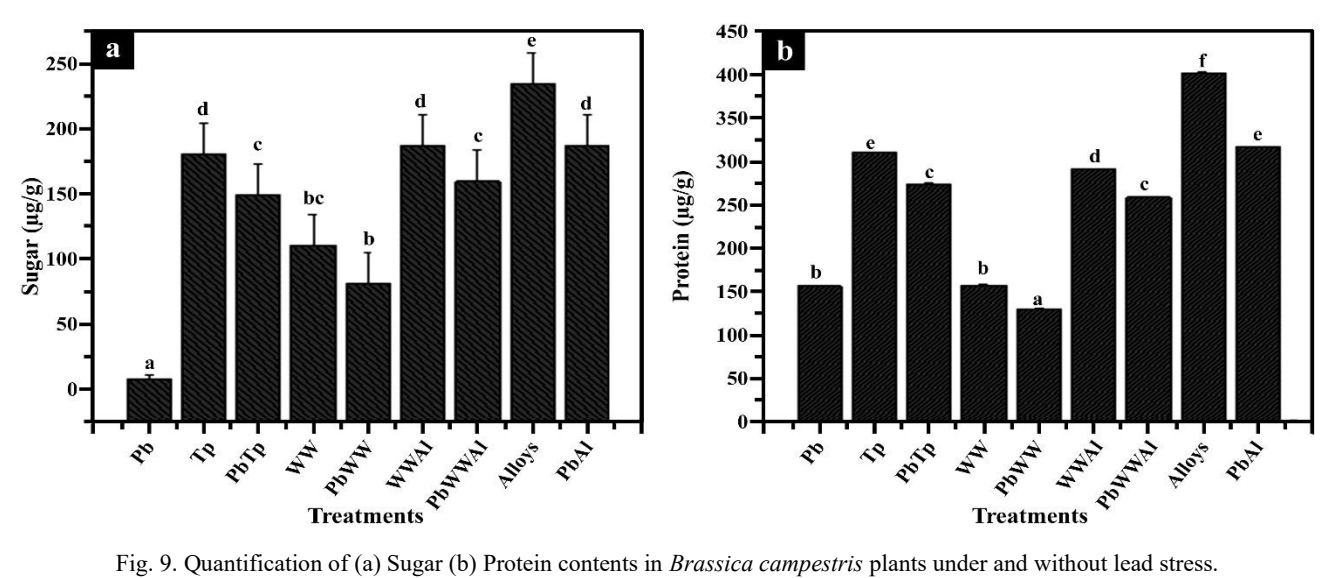


Fig. 9. Quantification of (a) Sugar (b) Protein contents in Brassica campestris plants under and without lead stress.

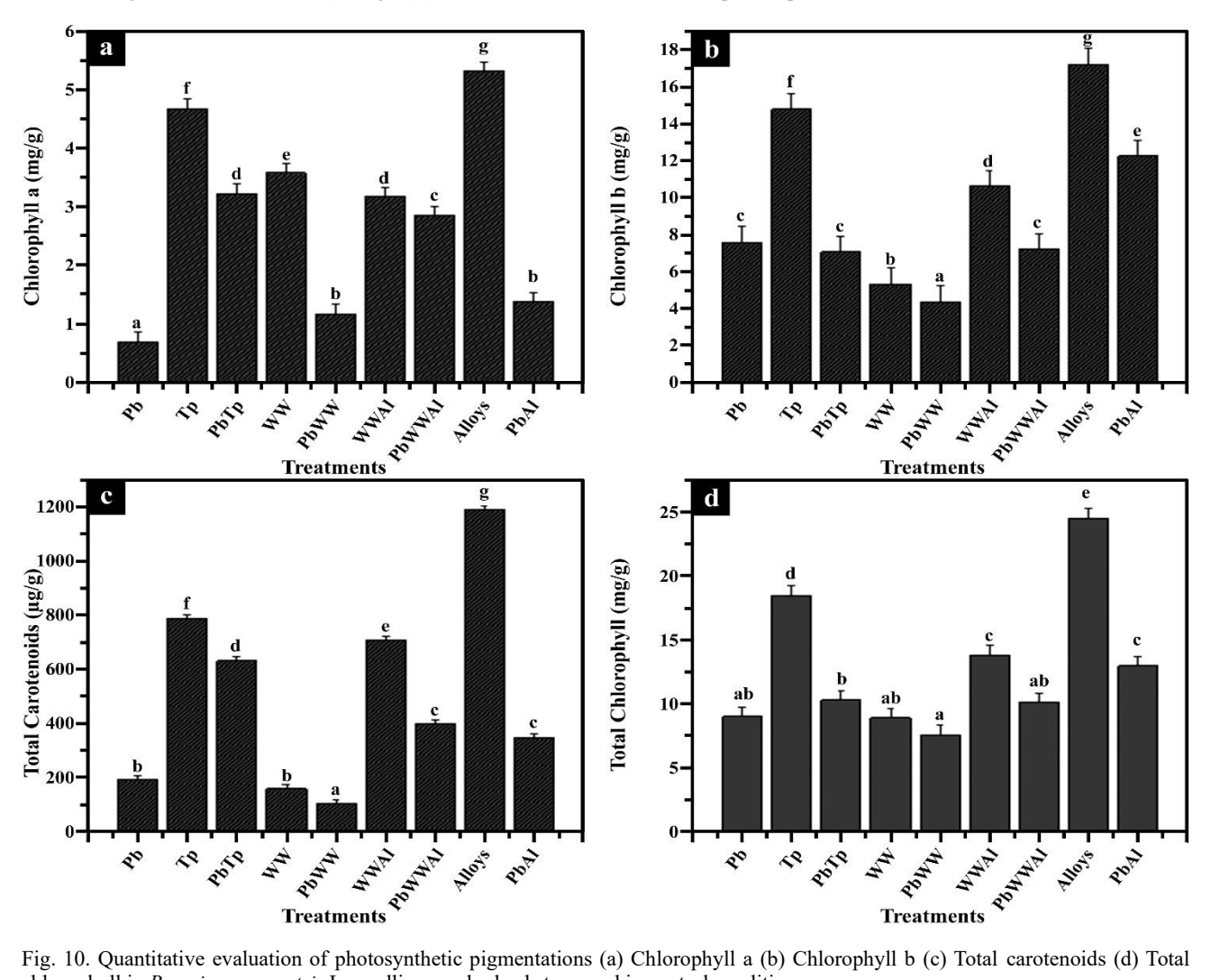


Fig. 10. Quantitative evaluation of photosynthetic pigmentations (a) Chlorophyll a (b) Chlorophyll b (c) Total carotenoids (d) Total chlorophyll in Brassica campestris L. seedlings under lead stress and in control condition.

Determination of catalase in Brassica campestris: Catalase levels under stress conditions caused by Pb, WWPb, and TpPb treatments were 1.37, 1.65, and 1.23 units/g, respectively. The treatments of AlPb and AlWPb alloys in stress have lowered the catalase level in comparison to other treatments. Catalase contents with no stressed condition were 0.51 units/g for alloys, 0.71 units/g for AlWW, WW, and tap water, and 0.6 units/g for tap water. Figure 11b shows the findings.

Determination of Lipid contents: Lipid levels were $61.23\mu g/g$, $64.71\mu g/g$, and 53.48 $\mu g/g$ under stress conditions brought on by Pb, WWPb, and TpPb treatments, respectively. Under stress, the alloys treated with AlPb and AlWPb had comparative lower lipid levels; 47.31µg/g and 43.51µg/g, respectively. Alloys with lipid content of 28.63 μg/g under non-stress conditions; AlWW, WW, and tap water showed 41.57 $\mu g/g$, 58.69 $\mu g/g$, and 38.47 $\mu g/g$, respectively. The results are displayed in figure 11c.

Determination of electrolytic leakage contents: The EL levels in the control group were TP (71), WW (58), AlWW (80), and alloy (84). The EL content dropped under stress, with Pb displaying 51, WWPb displaying 55, and TpPb displaying 56 levels of EL content. But compared to other treatments, alloys have high EL content under stress; AlPb (81EL) and AlWPb (74EL). Figure 11d presents these results.

Indole acetic acid: The use of alloys led to an increase in IAA. The following were the IAA levels that were seen for each treatment: The control group contained alloy as 365 $\mu g/g$, WWAl as 173 $\mu g/g$, tap water as 153 $\mu g/g$, and WW as 130 µg/g. Stress conditions resulted in significantly lower IAA levels: $65 \mu g/g$ for Pb, $114 \mu g/g$ for WWPb, and 143 µg/g for TpPb. Nevertheless, the use of alloys resulted in a higher IAA contents; AlPb observed 148 µg/g and AlWP 144 µg/g level of IAA in stressed condition as shown in the Fig. 12a.

Determination of GA3: In the control group, the GA3 levels for alloy (130 $\mu g/g$), WWAl (118 $\mu g/g$), Tap water (68 $\mu g/g),$ and WW (60 $\mu g/g)$ were observed. Under stressful conditions, Pb, WWPb, and TpPb were found to have drastically decreased to 8.5 μ g/g, 10.4 μ g/g, and 18.2 μg/g, respectively, of GA3. Nevertheless, the addition of alloys resulted in a higher GA3 content; under stress, AlPb displayed a level of 71.6 µg/g and AlWP exhibited 91.3 μ g/g (Fig. 12b).

Determination of ABA: Each treatment's ABA levels in the control group were as follows: Alloy (0.55 mg/g), WWA1 (0.158 mg/g), Tap water (0.34 mg/g), and WW (0.42 mg/g). Under stress, ABA levels were considerably lower: TpPb showed 0.13 mg/g, WWPb showed 0.05 mg/g, and Pb showed 0.09 mg/g. However, the amount of ABA increased with the usage of alloys; under stressful conditions, AlPb and AlWP showed 0.334 and 0.13 mg/g of ABA, respectively (Fig. 12c).

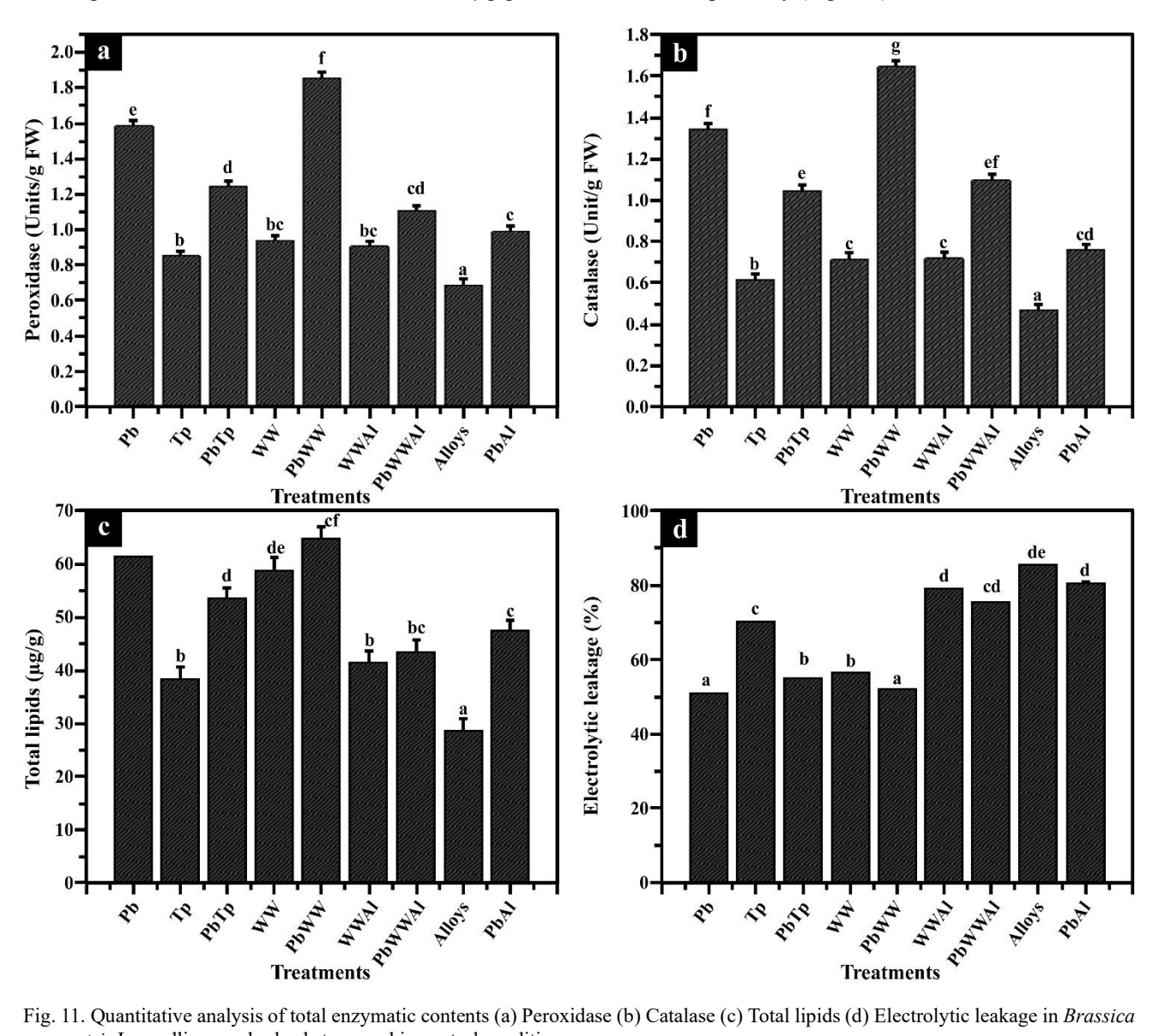


Fig. 11. Quantitative analysis of total enzymatic contents (a) Peroxidase (b) Catalase (c) Total lipids (d) Electrolytic leakage in Brassica campestris L. seedlings under lead stress and in control condition.

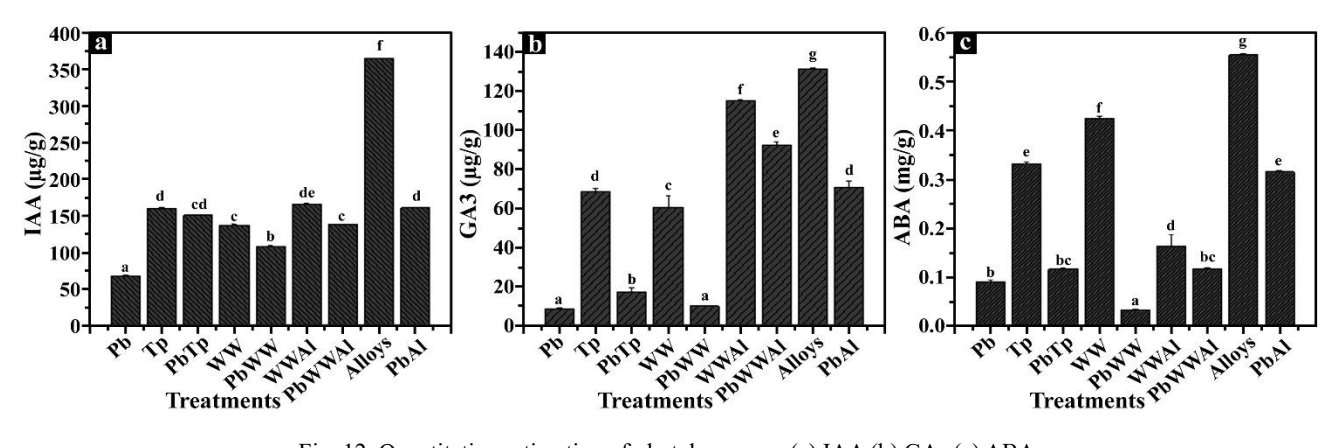


Fig. 12. Quantitative estimation of phytohormones (a) IAA (b) GA₃ (c) ABA.

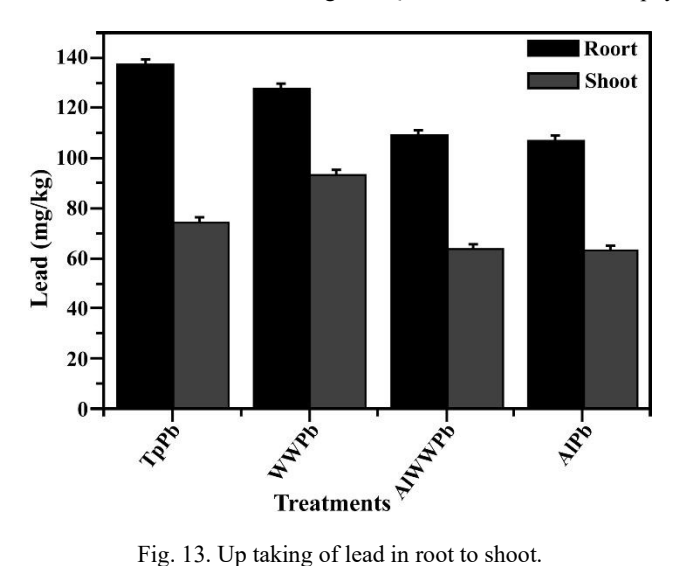


Fig. 13. Up taking of lead in root to shoot.

Lead concentration: The levels of lead in Brassica campestris roots and shoots after treatment with, wastewater, tap water and nanoparticles revealed prominent results. The Pb content in the shoots (93.04 mg/kg) and roots (127.6 mg/kg) increased significantly with WW (Pb). AlWW (Pb) and Alloys (Pb) roots and shoots had higher Pb levels, measuring 109.23 and 63.57 and 107.2 and 63.1 mg/kg, respectively (Fig. 13). Pb concentrations in the roots and shoots of the TP(Pb) treatment were found to be 137 and 74.05 mg/kg, respectively. Moreover, the addition of alloys (50 mg L⁻¹) resulted in a decrease in Pb levels in various tissues.

Discussion

Au-Ag nanoparticles hold promise for improving food safety and quality (Ghosh et al., 2023; Rahman et al., 2023). Alloys made with G. optiva leaf extracts showed the highest absorbance at 0.2 mL NaCl and the lowest at 1 mL. As NaCl increased, absorbance dropped-likely due to excess Cl⁻ ions encouraging the growth of larger particles and slowing reaction rates (Fig. 2d). Temperature also affected nanoparticle formation. Higher temperatures led to smaller particle sizes, sharper absorbance peaks, and increased nanoparticle concentration. This is because elevated temperatures accelerate the reaction, quickly consuming metal ions and reducing further growth. Stable high temperatures help limit aggregation and improve yield (Jamdagni et al.,

2018). In our study, the absorbance peak increased with temperature up to 65°C, after which it began to decline (Fig. 2e). This suggests that plant metabolites-like terpenoids and flavonoids-create ideal conditions for nanoparticle formation at this temperature (Sahni et al., 2015). These compounds, along with alkaloids, phenolic acids, steroids, and enzymes containing groups like -OH and -COOH, play a key role in the early stages of metal nanoparticle synthesis. Past studies have shown that such plant extracts act as natural reducing and stabilizing agents in forming both monometallic (Ag, Au) and bimetallic (Au-Ag) nanoparticles (Fig. 3) (Babu et al., 2022; Hunyh et al., 2020).

XRD analysis of the Ag-Fe alloy showed strong similarities to the patterns of individual Ag and Fe nanoparticles. Four distinct peaks appeared at 2θ values of 38.28°, 46.63°, 64.31°, and 77.27°, which correspond to the (111), (200), (220), and (311) crystal planes. These reflect the face-centered cubic structure typical of both Ag and Fe nanoparticles (Fig. 4). SEM imaging revealed that the synthesized alloy particles were mostly spherical and varied in size from 20 to 80 nm. Similar polydisperse and spherical structures were observed in nanoparticles synthesized using Amaryllis vittata extract. Some studies also noted monodisperse particles, likely due to enzyme immobilization (Sulthana et al., 2022). In addition, SEM images showed particle agglomeration in certain areas, likely caused by van der Waals forces between the nanoparticles (Ahmed et al., 2015) (Figs. 5A, 5B). TEM analysis showed that the biosynthesized Ag-Fe nanoparticles were mostly spherical and hexagonal, with an average size of about 14 nm (Alzahrani et al., 2022). The particles appeared evenly dispersed and varied in shape, as seen in histogram data (Fig. 5CD). Meanwhile, phytoremediation uses plants to reduce pollutants like metals, pesticides, and oil from contaminated sites (Kumar et al., 2023. Lead, being both mutagenic and carcinogenic, remains a major focus due to its serious health risks (Liévanos et al., 2021). Ag-Fe bimetallic nanoparticles improved shoot and root growth in Brassica campestris, while untreated or stressed wastewater reduced development (Fig. 7). Seedlings treated with alloys showed higher fresh and dry weights than those grown in plain tap or wastewater. Similar growth enhancement was observed in *Brassica juncea* at 25–50 ppm nanoparticle concentrations (Sharma et al., 2021; Fig. 8a). In Capsicum annuum, AgNPs-40 added to wastewater boosted biomass, countering heavy metal toxicity (Alomran et al., 2023; Singh et al., 2022; Fig. 8b). Wastewater reduced carbohydrates due to lower photosynthesis and nitrogen imbalance (Gondal et al., 2021). Heavy metal stress affected protein content, but Fe₃O₄ nanoparticles helped protect and preserve plant biomolecules (Singh *et al.*, 2021; Yaun *et al.*, 2021).

Peroxidase (POD), catalase (CAT), and antioxidant activities in leaves increased significantly under lead stress (WWPb) and wastewater treatment, while other dosages reduced enzyme activity (Figs. 12a-c). Soil treated with nanoparticles showed lower enzyme levels compared to control. Carrot plants irrigated with wastewater or treated with selenium nanoparticles showed enhanced antioxidant enzyme activity during stress (El-Batal et al., 2023). Stress conditions, especially with lead, raised lipid levels, but alloy treatments helped restore normal lipid content (Fig. 12d). Brassica napus and iron oxide nanoparticles effectively reduce heavy metal stress by maintaining lipid balance in plants (Shakoor et al., 2017; Singh et al., 2021). Irrigating with wastewater increased plants' tolerance to heavy metals, improving growth and photosynthesis (Anwar et al., 2016). Brassica campestris showed higher lead levels when treated with wastewater alone, while nanoparticle treatments reduced Pb uptake. Iron nanoparticles and S. aureus helped lower chromium absorption in plants (Alharby et al., 2022). Sewage sludge increased heavy metal uptake, especially cadmium and nickel (Singh & Agrawal, 2007). Nanoparticle composites, like iron and silver nanoparticles, improved crop yields and seed nutritional value without harm (Wu et al., 2023; Menhas et al., 2023).

Conclusion

Grewia optiva leaf extract was successfully employed in the nano-production of iron and silver nanoparticles as well as their alloys which resulted in favourable outcomes. Morphology and structure of the nanoparticles have been investigated in detail by a number of analytical methods including FT-IR, SEM, TEM, UV spectroscopy and XRD. For example, alloys relieved a particular stress and enhanced plant growth, in addition to the increased content of photosynthetic pigments like chlorophyll and carotenoids. Moreover, the pros include the fact that using Ag/Fe alloy phytoremediation is multifunctional. The growth of Brassica campestris, in a hydroponic experiment, was promoted via utilization of bimetallic nanoparticles in a bid to counteract the damaging effects of wastewater and lead on plant growth. As a result, there is a reduction in oxidative stress as well as an addition of primary and secondary metabolites in plants treated by biofabricated bimetallic particles. This means that the application of nanoparticles could counteract the damages to plants caused by heavy metal poisoning of the physiological and biochemical processes.

The results from the study point towards the effectiveness of nanophytoremediation, which states that if the nano-Ag and Fe nanoparticles or their composites (alloys) are exposed to the polluted water under the adequate conditions, the plants can remove the heavy metals from the water effectively. Therefore, this work results contribute to the expanding body of knowledge of nanoparticles use in the development of environmental remediation methods and provide concrete solutions to the heavy metal pollution problem and improvement of crops health and yield in contaminated areas. More research is needed in this field concerning the long-term effects and ecological repercussions of using nanoparticles in phytoremediation.

Acknowledgments

This project was funded by The Research Institute/Center Supporting Program (RICSP-25–3), King Saud University, Riyadh, Saudi Arabia.

References

- Acay, H. 2021. Utilization of Morchella esculenta-mediated green synthesis golden nanoparticles in biomedicine applications. *Biochem. Biotechnol.*, 51(2): 127-136.
- Ahmed, M.J., G. Murtaza, A. Mehmood and T.M. Bhatti. 2015. Green synthesis of silver nanoparticles using leaves extract of Skimmia laureola: characterization and antibacterial activity. *Mater. Lett.*, 153: 10-13.
- Alharby, H.F. and S. Ali. 2022. Combined role of Fe nanoparticles (Fe NPs) and Staphylococcus aureus L. in the alleviation of chromium stress in rice plants. *Life*, 12(3): 338.
- Alomran, M.M., A. Noman, N. Khalid, N. Hadayat, F.M. Alqahtani, F.M. Alzuaibr, N. Akhter, M. Hashem, T. Habeeb and O.M. Al-Zoubi. 2023. Harnessing melatonin protective efficacy in capsicum plants against nickel-contaminated soil. *J. Soil Sci. Plant Nutr.*, 1-13.
- Alzahrani, A.R., I.A.A. Ibrahim, N. Shahzad, I. Shahid, I.M. Alanazi, A.H. Falemban and M.F.N. Azlina. 2023. An application of carbohydrate polymers-based surface-modified gold nanoparticles for improved target delivery to liver cancer therapy-A systemic review. *Int. J. Biol. Macromol.*, 126889.
- Alzahrani, S., H. Ali, E.H. Althubaiti and M. Ahmed. 2022. Green synthesis of gold nanoparticles, silver nanoparticles and gold-silver alloy nanoparticles using Ziziphus spina-christi leaf extracts and antibacterial activity against multidrugresistant bacteria. *Ind. J. Pharm. Sci.*, 42-53.
- Anwar, N., A. Khan, M. Shah, A. Azam, K. Zaman and Z. Parven. 2016. The green synthesis of fine particles of gold using an aqueous extract of Monotheca buxifolia (Flac.). Russ. *J. Phys. Chem.*, 90: 2625-2632.
- Anwar, N., A. Khan, M. Shah, J.J. Walsh, S. Saleem, Z. Anwar, S. Aslam and M. Irshad. 2022. Hybridization of green synthesized silver nanoparticles with poly (ethylene glycol) methacrylate and their biomedical applications. *Peer J.*, 10: e12540.
- Anwar, S., M.F. Nawaz, S. Gul, M. Rizwan, S. Ali and A. Kareem. 2016. Uptake and distribution of minerals and heavy metals in commonly grown leafy vegetable species irrigated with sewage water. *Environ. Monit. Assess.*, 188: 1-9.
- Asad, S., N. Anwar, M. Shah, Z. Anwar, M. Arif, M. Rauf, K. Ali, M. Shah, W. Murad and G.M. Albadrani. 2022. Biological synthesis of silver nanoparticles by *Amaryllis vittata* (L.) Herit: From antimicrobial to biomedical applications. *Materials*, 15(16): 5478.
- Azmat, R., I. Altaf, S. Moin, W. Ahmed, A.F. Alrefaei and S. Ali. 2023. A study of photo-biological reactions under TiO2 nanoparticle accumulation in *Spinacia oleracea*. *Pak. J. Bot.*, 55: 1359-1364.
- Babu, P., S.R. Dash, A. Behera, T. Vijayaraghavan, A. Ashok and K. Parida. 2022. Prominence of Cu in a plasmonic Cu–Ag alloy decorated SiO 2@ S-doped C 3 N 4 core–shell nanostructured photocatalyst towards enhanced visible light activity. *Nanoscale Adv.*, 4(1): 150-162.
- Cruz, D.M., E. Mostafavi, A. Vernet-Crua, H. Barabadi, V. Shah, J.L. Cholula-Díaz, G. Guisbiers and T.J. Webster. 2020. Green nanotechnology-based zinc oxide (ZnO) nanomaterials for biomedical applications: a review. J. Phys. Mater., 3(3): 034005.
- El-Batal, AI., M.A. Ismail, M.A. Amin, G.S. El-Sayyad and M.S. Osman. 2023. Selenium nanoparticles induce growth and physiological tolerance of wastewater-stressed carrot plants.

- Biologia, 78(9: 2339-2355.
- Faiz, S., N.A. Yasin, W.U., Khan, A.A. Shah, W. Akram, A. Ahmad, A. Ali, N.H. Naveed and L. Riaz. 2022. Role of magnesium oxide nanoparticles in the mitigation of lead-induced stress in Daucus carota: modulation in polyamines and antioxidant enzymes. *Int. J. Phytoremed.*, 24(4): 364-372.
- Ghosh, S., S. Roy, J. Naskar and R.K. Kole. 2023. Plant-mediated synthesis of mono-and bimetallic (Au–Ag) nanoparticles: Future prospects for food quality and safety. *Journal of Nanomaterials*, 2023(1), p.2781667.
- Gondal, A.H., K. Tampubolon, M.D. Toor and M. Ali. 2021 Pragmatic and fragile effects of wastewater on a soil-plantair continuum and its remediation measures: a perspective. *Rev. Agric. Sci.*, 9: 249-259.
- Gorin, N. and F.T. Heidema. 1976. Peroxidase activity in Golden Delicious apples as a possible parameter of ripening and senescence. *J. Agric. Food Chem.*, 24(1): 200-201.
- Gulzar, A.B.M. and P.B. Mazumder. 2022. Helping plants to deal with heavy metal stress: the role of nanotechnology and plant growth promoting rhizobacteria in the process of phytoremediation. *Environ. Sci. Pollut. Res.*, 29(27): 40319-40341.
- Huynh, H.L., W.M. Tucho, X. Yu and Z. Yu. 2020. Synthetic natural gas production from CO2 and renewable H2: Towards large-scale production of Ni–Fe alloy catalysts for commercialization. J. Clean. Prod., 264: 121720.
- Jamdagni, P., P. Khatri and J.S. Rana. 2018. Green synthesis of zinc oxide nanoparticles using flower extract of Nyctanthes arbor-tristis and their antifungal activity. *J. King Saud Univ.* Sci., 30(2): 168-175.
- Khan, M., A.M. Khattak, S. Ahmad, S.A. Khalil, N. Ahmad, S.A.A. Shah, S. Ali, Y.S. Moon, M. Hamayun and A.F. Alrefaei. 2024. Polyethylene glycol-stimulated drought stress enhanced the biosynthesis of steviol glycosides in Stevia rebaudiana. *Pak. J. Bot.*, 56(5), pp. 1645-1652.
- Khan, N. and A. Bano. 2016. Role of plant growth promoting rhizobacteria and Ag-nano particle in the bioremediation of heavy metals and maize growth under municipal wastewater irrigation. *Int. J. Phytoremed.*, 18(3): 211-221.
- Khan, Z.I., E. Ugulu, A. Zafar, N. Mehmood, H. Bashir, K. Ahmad and M. Sana. 2021. Biomonitoring of heavy metals accumulation in wild plants growing at Soon Valley, Khushab, Pakistan. *Pak. J. Bot.*, 53(1): 247-252.
- Kumar, R., V. Verma, M. Thakur, G. Singh and B. Bhargava. 2023. A systematic review on mitigation of common indoor air pollutants using plant-based methods: a phytoremediation approach. Air Quality, Atmosphere & Health, 16(8): pp.1501-1527.
- Liévanos, R.S., L. Wilder, J. Richter Carrera and M. Mascarenhas. 2021. Challenging the white spaces of environmental sociology. *Environ. Sociol.*, 7(2): 103-109.
- Loza, K., Heggen and M. Epple. 2020. Synthesis, structure, properties, and applications of bimetallic nanoparticles of noble metals. Adv. Fun. Mater., 30(21): 1909260.
- Menhas, S., P. Zhou, S. Hayat, J. Bundschuh, T. Aftab, X. Chen, W. Liu and K. Hayat. 2023. Synergistic effect of melatonin in plant growth and development in stress mitigation. In: Melatonin in Plants: A Regulator for Plant Growth and Development. Springer: 245-266.
- Mofolo, M.J., P. Kdhila, K. Chinsembu, S. Mashele and M. Sekhoacha. 2020. Green synthesis of silver nanoparticles from extracts of Pechuel-loeschea leubnitziae: their antiproliferative activity against the U87 cell line. *Inorg. Nano-*

- Metal Chem., 50(10): 949-955.
- Mostafa, A.M. and E.A. Mwafy. 2020. The effect of laser fluence for enhancing the antibacterial activity of NiO nanoparticles by pulsed laser ablation in liquid media. *Environ. Nanotechnol. Monit. Manage.*, 14: 100382.
- Nizam, N.U.M., M.M. Hanafiah, E. Mahmoudi, A.W. Mohammad and A.A. Oyekanmi. 2022. Effective adsorptive removal of dyes and heavy metal using graphene oxide based pre-treated with NaOH/H2SO4 rubber seed shells synthetic graphite precursor: equilibrium isotherm, kinetics, and thermodynamic studies. Sep. Purif. Technol., 289: 120730.
- Rahman, A., G. Rehman, N. Shah, M. Hamayun, S. Ali, A. Ali and A.F. Alrefaei. 2023. Biosynthesis and characterization of silver nanoparticles using *Tribulus terrestris* seeds: Revealed promising antidiabetic potentials. *Molecules*, 28(10): 4203.
- Rajput, V.D., T. Minkina, A. Kumari, S.S. Shende, A. Ranjan, M. Faizan, A. Barakvov, A. Gromovik, N. Gorbunova, P. Rajput and A. Singh. 2022. A review on nanobioremediation approaches for restoration of contaminated soil. *Eurasian Journal of Soil Science*, 11(1): pp.43-60.
- Sahni, N., S. Yi, M. Taipale, J.IF. Bass, J. Coulombe-Huntington, F. Yang, J. Peng, Weile, G.I. Karras and Y. Wang. 2015. Widespread macromolecular interaction perturbations in human genetic disorders. *Cell*, 161(3): 647-660.
- Shakoor, A., M. Abdullah, R. Sarfraz, M.A. Altaf and S. Batool. 2017. A comprehensive review on phytoremediation of cadmium (Cd) by mustard (*Brassica juncea* L.) and sunflower (*Helianthus annuus* L.). J. Bioserv. Environ. Sci., 10(3): 88-98.
- Sharma, P., S. Tripathi and R. Chandra. 2021. Highly efficient phytoremediation potential of metal and metalloids from the pulp paper industry waste employing *Eclipta alba* (L) and *Alternanthera philoxeroide* (L): Biosorption and pollution reduction. *Biores. Technol.*, 319: 124147.
- Singh, A., D.B. Pal, S. Kumar, N. Srivastva, A. Syed, A.M. Elgorban, R. Singh and V.K. Gupta. 2021. Studies on Zero-cost algae based phytoremediation of dye and heavy metal from simulated wastewater. *Bioresour. Technol.*, 342: 125971.
- Singh, R. and M. Agrawal. 2007. Effects of sewage sludge amendment on heavy metal accumulation and consequent responses of Beta vulgaris plants. *Chemosphere*, 67(11): 2229-2240.
- Singh, S., J. Karwadiya, S. Srivastava, P.K. Patra and V. Venugopalan. 2022. Potential of indigenous plant species for phytoremediation of arsenic contaminated water and soil. *Ecol. Eng.*, 175: 106476.
- Sulthana, S., P. Kattel, J. Trousil, D. Pearson and S. Aryal. 2022, August. Synthesis and characterization of polymeric nanoparticles: effect of nanoparticle density in cellular compatibility and uptake. In 38th Annual Meeting, (p. 8).
- Wu, S., Y. Yang, Y. Qin, X. Deng, Q. Zhang, D. Zou and Q. Zeng. 2023. Cichorium intybus L. is a potential Cd-accumulator for phytoremediation of agricultural soil with strong tolerance and detoxification to Cd. J. Hazard. Mater., 451: 1311.
- Xu, W., T. Yang, S. Liu, L. Du, Q. Chen, X. Li, J. Dong, Z. Zhang, S. Lu and Y. Gong. 2022. Insights into the synthesis, types, and application of iron nanoparticles: the overlooked significance of environmental effects. *Environ. Int.*, 158: 106980.
- Yuan, L., P. Guo, S. Guo, J. Wang and Y. Huang. 2021. Influence of electrical fields enhanced phytoremediation of multimetal contaminated soil on soil parameters and plants uptake in different soil sections. *Environ. Res.*, 198: 111290.